International Journal of Nanomedicine

Dovepress
open access to scientific and medical research

Open Access Full Text Article

ORIGINAL RESEARCH

Controlled-release formulation of antihistamine based on cetirizine zinc-layered hydroxide nanocomposites and its effect on histamine release from basophilic leukemia (RBL-2H3) cells

International Journal of Nanomedicine downloaded from https://www.dovepress.com/
For personal use only.

This article was published in the following Dove Press journal:
International Journal of Nanomedicine
2 July 2012
Number of times this article has been viewed

Samer Hasan
Hussein Al Ali[1]
Mothanna Al-Qubaisi[2]
Mohd Zobir Hussein[1,3]
Maznah Ismail[2,4]
Zulkarnain Zainal[1]
Muhammad Nazrul Hakim[5]

[1]Department of Chemistry, Faculty of Science, [2]Laboratory of Molecular Biomedicine, Institute of Bioscience, [3]Advanced Materials and Nanotechnology Laboratory, Institute of Advanced Technology (ITMA), [4]Department of Nutrition and Dietetics, Faculty of Medicine and Health Science, Universiti Putra, Malaysia; [5]Department of Biomedical Science, Faculty of Medicine and Health Science, Universiti Putra Malaysia, Selangor, Malaysia

Abstract: A controlled-release formulation of an antihistamine, cetirizine, was synthesized using zinc-layered hydroxide as the host and cetirizine as the guest. The resulting well-ordered nanolayered structure, a cetirizine nanocomposite "CETN," had a basal spacing of 33.9 Å, averaged from six harmonics observed from X-ray diffraction. The guest, cetirizine, was arranged in a horizontal bilayer between the zinc-layered hydroxide (ZLH) inorganic interlayers. Fourier transform infrared spectroscopy studies indicated that the intercalation takes place without major change in the structure of the guest and that the thermal stability of the guest in the nanocomposites is markedly enhanced. The loading of the guest in the nanocomposites was estimated to be about 49.4% (w/w). The release study showed that about 96% of the guest could be released in 80 hours by phosphate buffer solution at pH 7.4 compared with about 97% in 73 hours at pH 4.8. It was found that release was governed by pseudo-second order kinetics. Release of histamine from rat basophilic leukemia cells was found to be more sensitive to the intercalated cetirizine in the CETN compared with its free counterpart, with inhibition of 56% and 29%, respectively, at 62.5 ng/mL. The cytotoxicity assay toward Chang liver cells line show the IC_{50} for CETN and ZLH are 617 and 670 µg/mL, respectively.

Keywords: cetirizine hydrochloric acid, nanocomposite, zinc-layered hydroxide, histamine release, rat basophilic leukemia (RBL-2H3) cells

Introduction

Nanocomposites are materials consisting of different phases, in which one of the phases has at least one dimension at the nanometer scale.[1] Layered double hydroxides (LDH) ($LDH - M^{2+}_{1-x}M^{3+}_{x}(OH)_2(A^{m-})_{x/m} \cdot nH_2O$) and layered hydroxide salts (LHS) ($LHS - M^{2+}(OH)_{2-x}(A^{m-})_{x/m} \cdot nH_2O$) are layered crystalline materials with unique properties, due to their easily exchangeable interlayer anionic species. The LDH and LHS layers are positively charged and derived from brucite, a magnesium hydroxide structure. Brucite layers are formed by centering magnesium ions, with two positive charges, between six octahedrally placed hydroxide groups. Each hydroxide is coordinated with three magnesium atoms.

Zinc-layered hydroxide (ZLH) is a layered hydroxide salt in which the zinc atoms are octahedrally coordinated with six hydroxide groups to give an empirical formula of $Zn_2(OH)_2(NO_3)_2 \cdot 2H_2O$, where the nitrate groups are coordinated directly with the zinc.[2] For the zinc hydroxide nitrate, with the empirical formula $Zn_5(OH)_8(NO_3)_2 \cdot 2H_2O$, and for the anhydrous form $Zn_5(OH)_8(NO_3)_2$, one quarter of the zinc atoms are located

Correspondence: Mohd Zobir Hussein
Department of Chemistry, Faculty of Science, Universiti Putra Malaysia, 43400 Serdang, Selangor, Malaysia
Tel +60 3 89466801
Fax +60 3 89435380
Email mzobir@science.upm.my

© 2012 Hussein Al Ali et al, publisher and licensee Dove Medical Press Ltd. This is an Open Access article which permits unrestricted noncommercial use, provided the original work is properly cited.

in tetrahedral sites above and below each empty octahedron and three of the vertices of the tetrahedron are occupied by a hydroxide ion shared with the octahedral sheet. The apex of the tetrahedron in the $Zn_5(OH)_8(NO_3)_2 \cdot 2H_2O$ structure is occupied by water and the nitrate ions are located between the layers surrounded by water molecules.[3] In the $Zn_5(OH)_8(NO_3)_2$ structure, the apex is occupied by nitrate ions and coordinates directly with the zinc tetrahedron.[2]

These materials can act as host matrices for the intercalation of organic drugs and bioactive compounds for the formation of so-called nanocomposites. In addition, layered nanocomposite materials usually show high biocompatibility, few adverse reactions, and have good half-lives, which subsequently decrease drug side effects and improve the solubility of drugs with controlled-release capability.[4]

The size and shape of nanocomposites are very important, especially for biomedical applications. It has been reported that a nanocomposite with a size of 100–200 nm is suitable for use as a drug delivery vector.[5] However, a nanocomposite that is too small cannot reach the ideal state because of its high surface activity and small drug-loading capacity.[6] Layered nanocomposites can be used directly for cellular delivery without further modification to improve cellular uptake of biomolecules and drugs.[7] As the cellular internalization of drugs with a negative charge is inhibited because of the negative charge of cell walls, the intercalation of drugs into the interlayer of the host will neutralize the surface charge of anionic drugs due to the cationic charge of the layer, which leads to favorable endocytosis of cells, and results in enhanced transfer efficiency.[8] Previous work has shown that the efficacy of doxorubicin toward tumor cells was increased after the drug was intercalated into LDH compared with its free counterpart.[9]

Various compounds, such as gallic acid,[10] ellagic acid,[4] hippuric acid,[11] linoleic acid,[12] 2- and 4- amino benzoic acid[13] and various pharmaceutical, cosmeceutical, and nutraceutical compounds,[14] have been intercalated into ZLH. This intercalation can occur via various routes, such as the hydrolysis of urea in the presence of zinc nitrate solution,[3] the hydrolysis of metal salts in the presence of metal oxide,[15] precipitation using alkaline solutions,[16] and solid state reactions.[17]

Histamine is a normal constituent of mammalian tissue,[18] synthesized by the decarboxylation of histidine, and stored in tissue mast cells and basophilic granulocytes in the blood. Release occurs in response to tissue injury or allergic reactions.[18] H1, H2, and H3 are histamine receptors. Cetirizine dihydrochloride ({2-[4-[(4-chlorophenyl)-phenylmethyl]-1-piperazinyl] ethoxy} acetic acid), which is one of the second-generation antihistamines, displaces histamine from the H1 receptor. This leads to the formation of inositol 1, 4, 5-tris phosphate and a release of stored Ca^{+2}. In addition to cetirizine, zinc can also prevent this activity and lead to a decrease in Ca^{+2} inside the cell.[19,20]

In the present work, we have selected cetirizine as a model drug to be intercalated into ZLH using zinc oxide as the starting material. We focused our work on the structure, as well as the thermal and controlled-release properties of the as-synthesized drug-ZLH nanocomposite, with the intention of using this nanocomposite for controlled-release antihistamine delivery. The effect of the cetirizine nanocomposite (CETN) and ZLH on histamine release from rat basophilic leukemia (RBL-2H3) cells will also be studied.

Materials and method

Materials

Cetirizine hydrochloric acid (CET) ($C_{21}H_{25}ClN_2O_3 \cdot 2HCl$, molecular weight 461.5) was purchased from Upha Pharmaceutical Manufacturing (Selangor, Malaysia) with 99.9% purity and used as received. Zinc oxide (reagent grade), purchased from Fisher Scientific (Waltham, MA), sodium hydroxide (NaOH), phosphate buffer solutions, and Trypan blue purchased from Sigma-Aldrich (St Louis, MO), and deionized water were used in all experiments.

Preparation of CETN

CETN was synthesized directly from zinc oxide as the starting material, using methods similar to those previously described.[11,21] Cetirizine solution (0.04 mol/L) was prepared by dissolving 1.8 g cetirizine in 100 mL of water. Zinc oxide powder (0.2 g) was suspended in 50 mL of water. Cetirizine solution was added dropwise to the zinc oxide suspension with vigorous stirring; after the addition was complete, the solution became clear. This was followed by the addition of NaOH (0.125 mol/L) until the pH reached 7.9. The resulting slurry was aged at 70°C for 18 hours, then centrifuged and washed with deionized water, dried in an oven at 60°C, and kept in a sample bottle for further use and characterization.

Characterization

Powder X-ray diffraction patterns were recorded with a Shimadzu XRD-6000 (Shimadzu Corporation, Kyoto, Japan) instrument in the range of 2–60° using CuK_α radiation (λ = 1.5418 Å) at 30 kV and 30 mA, with a dwell time of 0.5°/min. Fourier transform infrared (FTIR) spectra of the materials were recorded over the range of 400–4000 cm^{-1} on a Thermo Nicolet Nexus, Smart Orbit spectrometer using a

sample of approximately 1% in 200 mg of spectroscopic grade KBr, with 10 tons of pressure. The elemental analysis (carbon, hydrogen, and nitrogen) in the cetirizine and its nanocomposite was obtained with a CHNS-932 from LECO Instruments (St Joseph, MI). The percentage of zinc in the nanocomposite was obtained using atomic absorption spectroscopy, performed on a Thermo Elemental Model S4 (Thermo Scientific, Walthm, MA) instrument. Thermal degradation studies (thermogravimetric and differential thermogravimetric analyses [TGA/DTG]) were performed using a Metter-Toledo 851e instrument (Switzerland) with a heating rate of 10°C/min, in the range of 20°C–1000°C, under a nitrogen atmosphere (N_2 flow rate 50 mL/min). Surface study of the materials was carried out using a nitrogen gas adsorption–desorption technique at 77 K with a Micromeritics ASAP2000 (Norcross, GA). The sample was degassed in an evacuated-heated chamber at 105°C for 6 hours. The surface morphologies of the samples were observed using a NOVA™ NanoSEM 230 (FEI, Hillsboro, OR) scanning electron microscope. UV-Vis spectra were measured to determine the optical properties and a controlled release study, using an ultraviolet-visible spectrophotometer (Perkin Elmer. Waltham, MA).

Loading and release amounts of cetirizine in CETN

The loading amount of cetirizine in the CETN was determined using a Perkin-Elmer Lambda 35 UV-visible spectrophotometer. A known weight of CETN was placed in a 10 mL volumetric flask, and 0.5 mL of 1 mol/L HCl solution was added. The concentration of cetirizine in the solution was determined at 231 nm using the standard curve of a series of standard solutions of known cetirizine concentration.

The release of cetirizine from CETN into the medium of phosphate buffer solution at pH 7.4 and pH 4.8[22–24] was achieved by adding about 85 mg of CETN into 250 mL buffer solutions. The accumulated amount of cetirizine released into the solutions was measured at different times using a UV-visible spectrophotometer at 231 nm. To compare the release rate of cetirizine from CETN with that from the physical mixture of cetirizine and pristine ZLH (ZLH was prepared for this purpose),[16] the same cetirizine-release experiments were performed with 0.6 mg of the physical mixture containing cetirizine (0.3 mg) and the pristine ZLH (0.3 mg).

Cytotoxicity assay

In a typical cytotoxicity assay, Chang cells line were first seeded into six-well plates when they reached 90% confluence and allowed to incubate overnight at 37°C in a 5% CO_2 atmosphere. After incubation for 24 hours for cell attachment, the medium was removed and replaced with 3 mL of the fresh growth medium containing different amounts of ZLH and CETN nanomaterials, from 7.8 to 1000 µg/mL. A control experiment was performed without treatment under the same conditions. The plates were incubated at 37°C, in 5% CO_2, for 24 hours. After incubation, the media was aspirated off and the cells were harvested by centrifugation then washed with cold phosphate buffered saline. 10 µL of cells was mixed with equal volume of 0.4% trypan blue and was counted using Neubauer hemocytometer (Weber, England) by clear field microscopy (Nikon, Japan). Only viable cells were counted. Each compound and control was assayed in triplicate.

Cell culture conditions and anti immunoglobulin (Ig) E-induced histamine release

RBL-2H3 cells were obtained from the American Type Tissue Collection (Rockville, MD). These cells were grown in Dulbecco's modified Eagle's medium, which was supplemented with 10% fetal bovine serum. The media contained penicillin (100 U/mL) and streptomycin (100 µg/mL). Cells were grown at 37°C in a humidified 5% CO_2 incubator.

For the determination of histamine release, the RBL-2H3 cells were plated at 1×10^6 cells/well by adding 0.5 mL of a 2×10^6 cells/mL suspension to each well of a 24-well tissue culture plate and incubated for 18 hours to assure attachment and 90% confluence. After the media was aspirated away, IgE (0.2 µg/mL; MP Biomedicals, Illkirch, France) was added to the Dulbecco's modified Eagle's medium. Cells were incubated at 37°C for 1 hour. Subsequently, each well was washed with release buffer (1 mM $CaCl_2$, 40 mM NaOH, 0.1% BSA, 119 mM NaCl, 5 mM KCl, 5.6 mM glucose, 25 mM piperazine-N, N-bis (2-ethanesulfonic acid) (PIPES), and 0.4 mM $MgCl_2$). Release buffer containing anti-IgE (1.25 µg/mL) and different concentrations of cetirizine, CETN, and ZLH were then added to each well and the cells were incubated at 37°C for 10 minutes. The amount of released histamine was determined using a histamine Radio immuno assay (RIA) kit (MP Biomedicals, Illkirch, France).

Results and discussion

Powder X-ray diffraction and structural model

Figure 1 illustrates the powder X-ray diffraction patterns of (A) zinc oxide, (B) CETN, and (C) cetirizine. For the pure

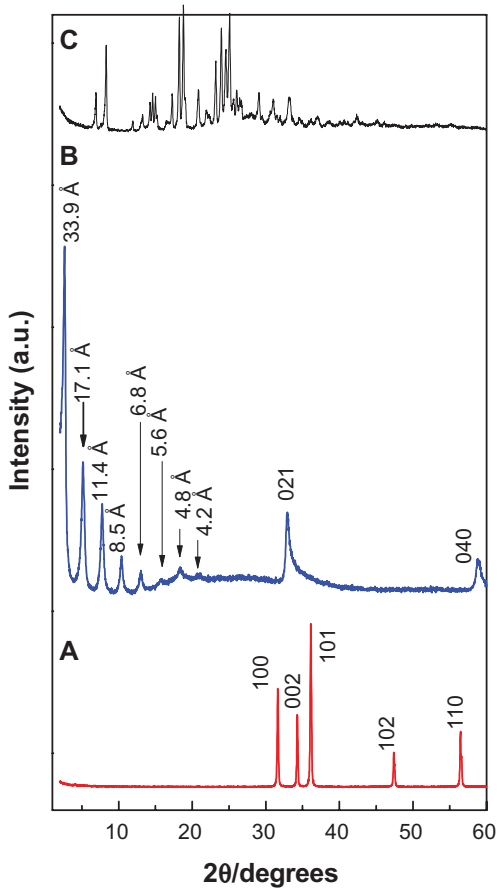

Figure 1 Powder X-ray diffraction patterns of (**A**) zinc oxide, (**B**) CETN, and (**C**) cetirizine.
Abbreviation: CETN, cetirizine nanocomposite.

zinc oxide sample, five intense peaks between 30° and 60° can be observed, which correspond to diffractions due to the 100, 002, 101, 102, and 110 planes. The intercalation process was undertaken by mixing an aqueous solution of cetirizine anions with the starting material, zinc oxide. The intercalation occurred when the zinc oxide was transformed to ZLH and cetirizine was intercalated between the layers. This can be observed by the disappearance of the reflections of the zinc oxide phase and a simultaneous sharp intense peak at a low 2θ angle, with d spacing of 33.9 Å (an average of eight harmonics). This indicates successful intercalation of cetirizine into the interlayers of ZLH (Figure 1B). In addition, Figure 1B shows another seven harmonics at 2θ = 5.16°, 7.75°, 10.38°, 13.01°, 15.79°, 18,36°, and 21.04° with d values of 17.1, 11.4, 8.5, 6.80, 5.60, 4.8 Å and 4.2 Å, respectively, resulting in an average d value of 33.9 Å. The peaks at 2θ = 32.98° and 58.77° with d values of 2.7 and 1.57 Å are related to the 021 and 040 planes, respectively.[25] The formation of CETN synthesized by direct reaction of zinc oxide in an aqueous environment is believed to occur through a dissociation–deposition mechanism.[21,26]

Figure 2 shows the three ionizable forms of cetirizine: a strong acidic group with $pK_2 = 2.9$, a strong basic group with $pK_3 = 8.0$, and a very weakly basic group with $pK_1 = 2.2$.[27] Figure 2A is the neutral form of cetirizine, which is absent in any pH medium. The anionic form of cetirizine (Figure 2B) is present in media at pH 10. At pH 7.9–8.0, cetirizine is found in anionic (2B) and zwitterion forms (2C) in equal amounts.[27] The pH used in this work was 7.9; therefore, the structural model for cetirizine was thought to be the anionic and zwitterion forms. Using ChemOffice software 2008 (Cambridge, MA), the long and short axes, and the molecular thickness of cetirizine were calculated to be 16.2, 8.5, and 11.8 Å, respectively, for the anionic form, and 16.2, 8.0, and 11.8 Å, respectively, for the zwitterion form. The dimensional difference between the two forms is only in the short axis. Using the average basal spacing of 33.9 Å for cetirizine,

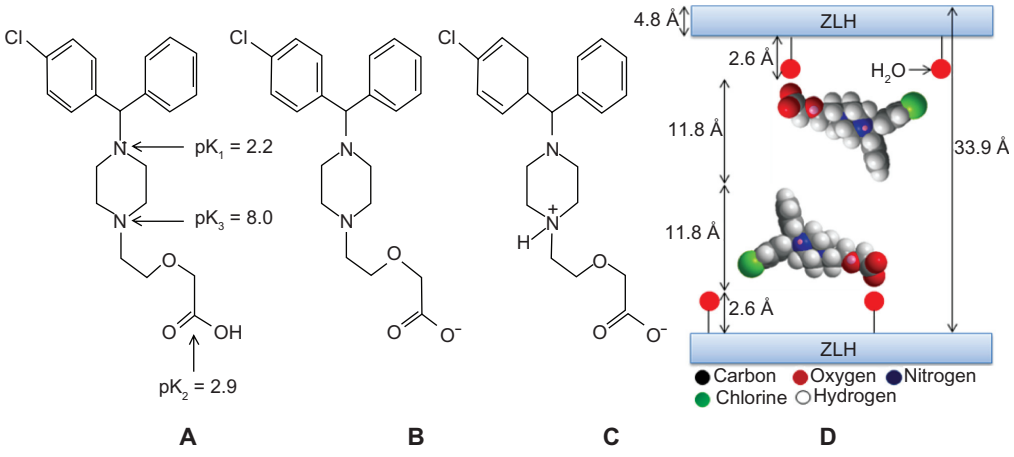

Figure 2 Structure of cetirizine at different pH (**A**–**C**) and molecular structure model of cetirizine intercalated between the interlayer of ZLH (**D**).
Abbreviation: ZLH, zinc-layered hydroxide.

observed by X-ray diffraction, and subtracting the thickness of the brucite layer (4.8 Å) and 2.6 Å for each zinc tetrahedron,[3] the gallery height was calculated to be 23.9 Å, which is nearly twice the thickness of cetirizine. Therefore, it is proposed that cetirizine molecules are arranged in a bilayer, as shown in Figure 2D.

FITR spectroscopy

FTIR spectra of pure cetirizine and CETN are shown in Figure 3 and the absorption bands are listed in Table 1. Figure 3A shows the spectrum for cetirizine. There are three different bands for the OH group: stretching vibration at 3432 cm^{-1}, dimmer at 2379–2628 cm^{-1}, and OH bending between 1284 and 1242 cm^{-1}.[29] A band due to C-H stretching of the aromatic ring was recorded at 3044–3023 cm^{-1}. Bands at 2984–2949 cm^{-1} are attributed to CH_2 stretching. A strong band at 1740 cm^{-1} is attributed to the stretching of the C=O group of the carboxylic group. Bands between 1435 and 1319 cm^{-1} are attributed to the C–O carboxylic bond. A stretching of the C–Cl bond appeared at 1457 cm^{-1}. Monosubstitution on the benzene ring gives three different

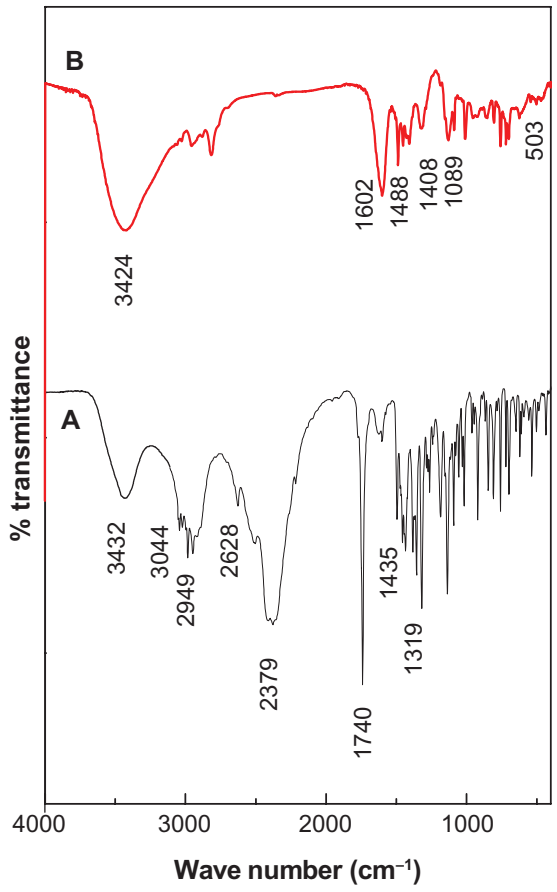

Figure 3 Fourier transform infrared spectra of (**A**) cetirizine and (**B**) the cetirizine nanocomposite.

Table 1 Fourier transform infrared assignment for cetirizine and CETN[21,29]

Assignments	Cetirizine	CETN
ν (O–H)	3432 for O–H in carboxylic group	3424 in the layer; H_2O
ν (CH_{ar})	3044–3023	–
ν (CH_2)	2984–2949	2958–2817
ν (OH) dimmer	2628, 2505 and 2379	–
ν (NH^+) cyclic	2217	–
ν (COOH)	1740	–
ν (ϕ. parasubst)	1601	1602
ν (ϕ. monosubst)	1496, 1077 and 758	1488
ν (C–Cl)	1457	1453
ν (C–O) in carboxylic group	1435, 1383, 1356 and 1319	–
δ (O–H)	1284, 1274, 1263 and 1242	–
δ (CH_2 CH_2O CH_2)	1185	1130
2 adj ϕ	846 and 809	853 and 804
ν (CH monosubst)	758	758
Zn–O and Zn–OH	–	503
$\nu_{as}(COO^-)$	–	1602
$\nu_s(COO^-)$	–	1408

Abbreviations: adj, adjacent; CETN, cetirizine nanocomposite; monosubst, monosubstitution; parasubst, parasubstitution.

absorption bands, 1496, 1077, and 758 cm^{-1}. Substitution at the para position on the benzene ring gives a band at 1602 cm^{-1}. A band at 1185 cm^{-1} is due to the CH_2 CH_2OCH_2 bending. Two adjacent benzene rings give bands at 846–809 cm^{-1}.

Figure 3B indicates that some characteristic absorption peaks of pure cetirizine at 1601, 1453, 1130, 853, 804, 758, and 719 cm^{-1} are slightly shifted due to the interaction between the cetirizine and the positively charged inorganic-host interlayers (Table 1). This shift indicates the presence of cetirizine anions between the layers of ZLH. The FTIR spectrum of the nanocomposite is thus slightly different from that of pure cetirizine. The characteristic C=O stretching vibration of the carboxylic group at 1740 cm^{-1} has vanished in the nanocomposite. This result indicates that cetirizine in the nanocomposite interlayer takes the form that has a negatively charged oxygen (Figure 2B). The intense peaks at 1601 cm^{-1} and 1408 cm^{-1} are due to asymmetric and symmetric stretching of the COO– group, respectively.[30,31] A band at 700 cm^{-1} can be attributed to OH bending within the layers. Two bands at 503 and 436 cm^{-1} are attributed to the Zn–OH and Zn–O lattice vibrations.[25]

Thermal study

The thermogravimetric and differential thermogravimetric analyses obtained for cetirizine and CETN are shown in Figure 4. The greatest weight loss for cetirizine (Figure 4A)

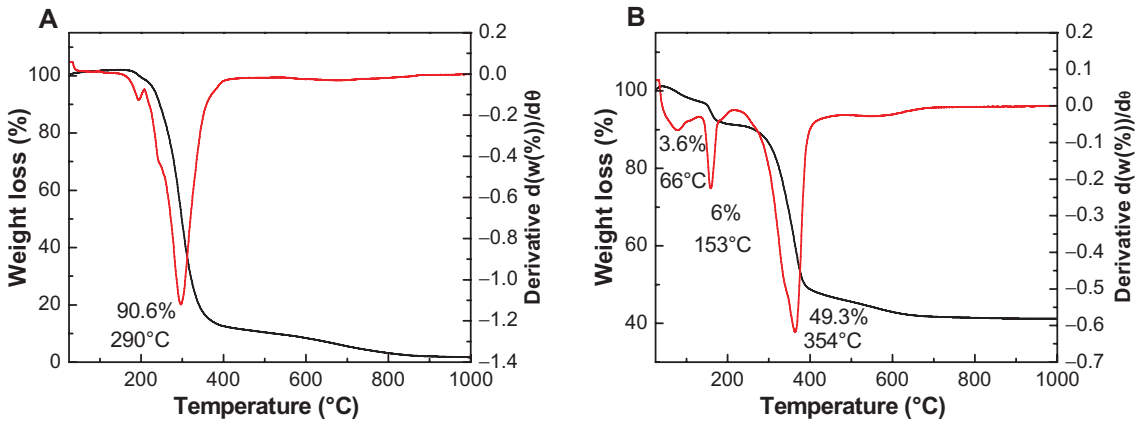

Figure 4 Thermogravimetric and differential thermogravimetric analyses of (**A**) cetirizine and (**B**) the cetirizine nanocomposite.

occurred between 159°C and 435°C with a total weight loss of 90.6%. There was a very small weight loss from 159°C to 210°C, due to the evolution of hydrochloric acid.[29] Weight loss stopped at 800°C due to the vaporization of the remaining cetirizine material.

Figure 4B shows three weight losses for CETN with temperature maxima at 66°C, 153°C, and 354°C, corresponding to weight losses of 3.6%, 6.0%, and 49.3%, respectively. The first weight loss was due to the removal of surface-physisorbed water molecules. The second weight loss in the range of 123°C–205°C was due to the removal of water molecules from the intercalated structure.[32] The third weight loss was due to dehydroxylation of the layers together with the decomposition of cetirizine, yielding zinc oxide as a residue.[33] Increasing the decomposition of cetirizine from 159°C (for free cetirizine) to 219°C (for cetirizine intercalated into the nanocomposite) indicates the greater thermal stability of cetirizine in CETN than as the unbound compound. The third weight loss, shown in Figure 4B, is in agreement with the elemental analysis result (Table 2), which shows that the loading percentage of cetirizine in the nanocomposite is 49.4% and CETN contains 32.1% carbon, 4.1% hydrogen, and 3.5% nitrogen.

Surface characterization

Figure 5A shows the adsorption–desorption isotherms for zinc oxide and CETN. According to the International Union of Pure and Applied Chemistry classification for the types of adsorption–desorption isotherms, zinc oxide and CETN are Type IV, mesoporous materials (Figure 5A). The N_2 adsorbate uptake for zinc oxide is slow in the relative pressure range of 0.0–0.8. After that, the adsorption increases rapidly to reach an optimum uptake of about 8 cm^3/g, which is a low uptake of nitrogen gas. Similarly, CETN also shows a Type IV isotherm. The adsorption increases slowly at low relative pressure in the range of 0.0–0.7, followed by rapid uptake of the adsorbate at a relative pressure > 0.7, and reaches an optimum of 460 cm^3/g. The desorption branch of the hysteresis loop for CETN is much broader compared with zinc oxide due to differences in the texture of the latter. Table 2 shows the surface area of the materials as determined by the Brunauer, Emmett, and Teller (BET) method. Due to a decrease in the pore size and an increase in the pore volume, the surface area increased from 6 m^2/g for zinc oxide to 24 m^2/g for CETN. This also indicates a change in the pore texture because of the formation of the CETN compound.

Figure 5B shows plots of the Barrett–Joyner–Halenda (BJH) desorption pore-size distribution for zinc oxide and CETN. As shown in the figure, zinc oxide gives a single-peak pore-size distribution centered at around 33 Å, while the pore size distribution for CETN is centered at 140 Å. Table 2 shows the average pore diameter and

Table 2 Physico-chemical properties of zinc oxide and the cetirizine nanocomposite (CETN)

Sample	C (%)	H (%)	N (%)	Zn (% w/w)	Anion (% w/w)	BET surface area m^2/g	BJH pore volume cm^3/g	BJH average pore diameter Å
ZnO	–	–	–	(80.3)	–	6	0.01	111
CETN	32.1	4.1	3.5	32.3[b]	49.4[a] (47.3[c])	24	0.71	96

Notes: Value in the parentheses is a theoretical value. [a]Estimated from carbon, hydrogen, nitrogen and sulfur analysis data; [b]estimated from atomic absorption spectroscopy analysis; [c]estimated from UV.

Abbreviations: BET, Brunauer, Emmett, and Teller method; BJH, Barrett–Joyner–Halenda method; ZnO, zinc oxide; CETN, cetirizine nanocomposites.

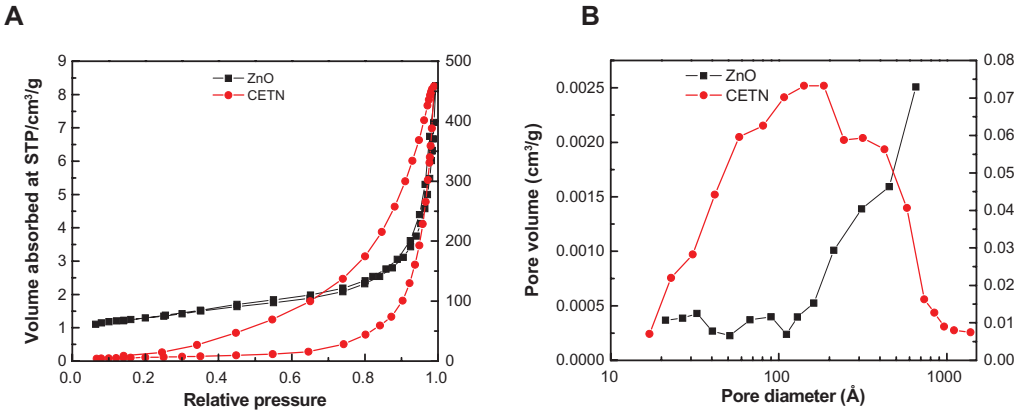

Figure 5 Adsorption-desorption isotherms for zinc oxide and CETN (**A**) and Barret–Joyner–Halenda method pore size distribution for zinc oxide and CETN (**B**).
Abbreviation: CETN, cetirizine nanocomposite.

pore volume determined by BJH. The BJH average pore diameter decreased from 111 for zinc oxide to 96 Å for CETN, respectively. The BJH desorption pore volume increased from 0.01 cm^3/g for zinc oxide to 0.71 cm^3/g for CETN.

The surface morphology of zinc oxide and CETN are shown in Figure 6. The micrographs were obtained using a field emission NOVA™ NanoSEM 230 (FEI, Hillsboro, OR) scanning electron microscope, at (A and C) 25,000× and (B and D) 50,000× magnifications. Zinc oxide shows various sizes and has a nonuniform granular structure without any specific shape (A and B). Formation of CETN resulted in a morphology change to agglomerates of compact and non-porous granular structure (C and D).

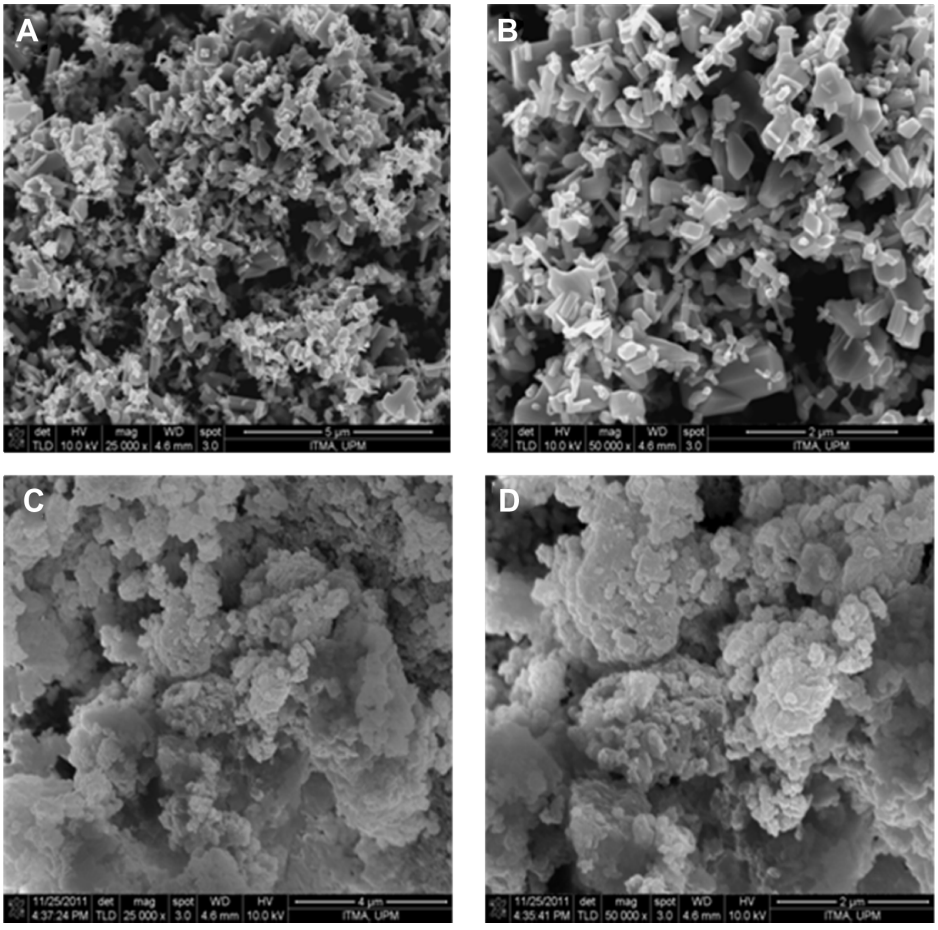

Figure 6 Field emission scanning electron microscope image of zinc oxide (**A** and **B**) and the cetirizine nanocomposite (**C** and **D**).

Release behavior of cetirizine

To study the release behavior of cetirizine from CETN and its physical mixture, the samples were individually dispersed in phosphate buffer solutions at pH 7.4 and 4.8. Absorbance was recorded at different time intervals. The release curve for the physical mixture of cetirizine and pristine ZLH in buffer solutions at pH 7.4 and 4.8 are shown in Figure 7C and D, respectively. These figures show that cetirizine is rapidly released from the physical mixture and release is complete within 8 minutes at pH 7.4 and 3 minutes at pH 4.8. The release rate of cetirizine from CETN (Figure 7II (A and B)) was obviously much slower than that from the physical mixture. This is attributed to the electrostatic attraction between cetirizine anions and the ZLH inorganic interlayer together with the ion-exchange property. This result indicates that CETN has potential in a controlled-release formulation of the antihistamine.

Figure 7II (A and B) show the release profiles of cetirizine from CETN into phosphate buffer solution at pH 7.4 and 4.8. The release rates in both media were remarkably dependent on the acidity of the buffer; the total amount of cetirizine released from CETN reached 97% within about 73 hours at pH 4.8, compared with the slower release rate of cetirizine at pH 7.4, where the time taken for 96% to be released was 83 hours.

Figure 7I (A and B) show the release profiles for cetirizine into the buffer solutions for the first 5 hours at pH 7.4 and 4.8. It was found that the release is very rapid for the first 5 minutes with 15% release at pH 7.4 compared with 40% at pH 4.8. This phenomenon is presumably due to the "burst effect"[34] and other mechanisms, depending on the acidity of the media. The burst effect occurs due to the high release of cetirizine anions at the first start (about 3% w/w) adsorbed on the ZLH surface, a conservative estimate from the observed pure phase powder X-ray diffraction pattern of the nanocomposite. A slower one thereafter followed the release (79% at pH 7.4 and 86% at pH 4.8 after 5 hours). The difference in the release rates at pH 4.8 and 7.4 is mostly due to the difference in release mechanism.[35] At acidic pH (4.8), the release mechanism possibly follows the dissolution of ZLH interlayers and ion exchange. This is due to the fact that ZLH is not stable in acidic media and begins to dissolve. Thus, release of an interlayer molecule should occur mainly because of the removal of the inorganic host. However, at pH 7.4, the ZLH is more stable and as a result, the mechanism should be through ion exchange with the ions in the buffer solution.[35] The motion of cetirizine is restricted due to the steric effect of ZLH and there is electrostatic interaction between cetirizine anions and the positively charged ZLH interlayers. Release profiles for cetirizine from CETN (Figure 7I) show results similar to those of other drugs, such as 5-flurouracil, camptothecin, naproxen, l-Dopa, and 5-florocytosine, found in the literature.[22,24,35–38]

Release kinetics of cetirizine from CETN

In order to better understand the mechanism of the release of cetirizine from CETN, the results of the kinetic studies were analyzed using pseudo-first order (Equation 1),[39] pseudo-second order (Equation 2),[40] and parabolic diffusion (Equation 3)[41] equations:

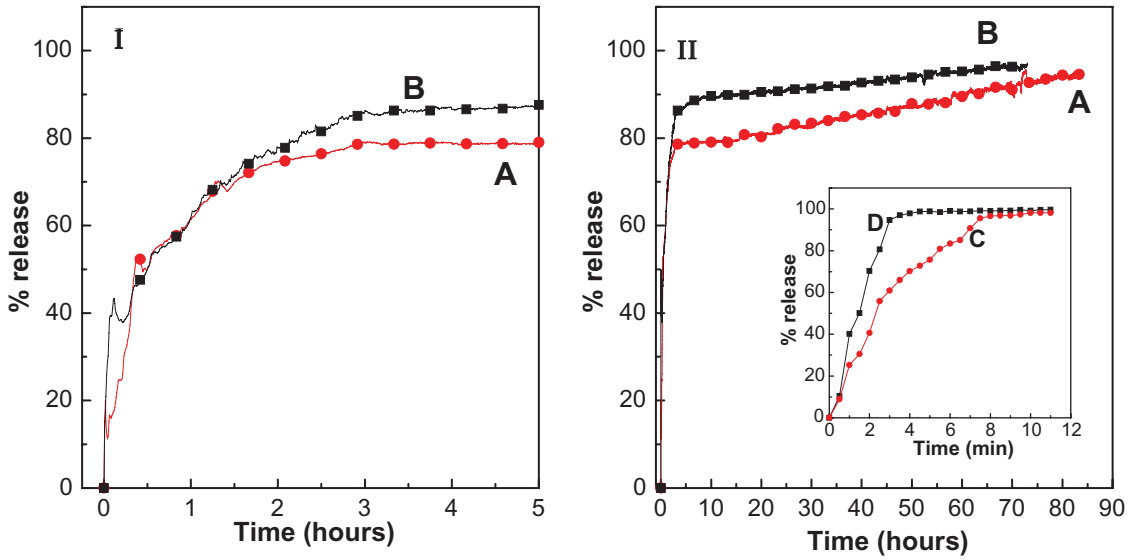

Figure 7 (**I**) Release profiles of cetirizine from the cetirizine nanocomposite at pH 7.4 (**A**) and pH 4.8 (**B**) up to 5 hours; (**II**) release profiles of cetirizine up to 83 hours.
Note: Inset shows the release profiles of cetirizine from its physical mixture of cetirizine with zinc layered hydroxide at pH 7.4 (**C**) and pH 4.8 (**D**).

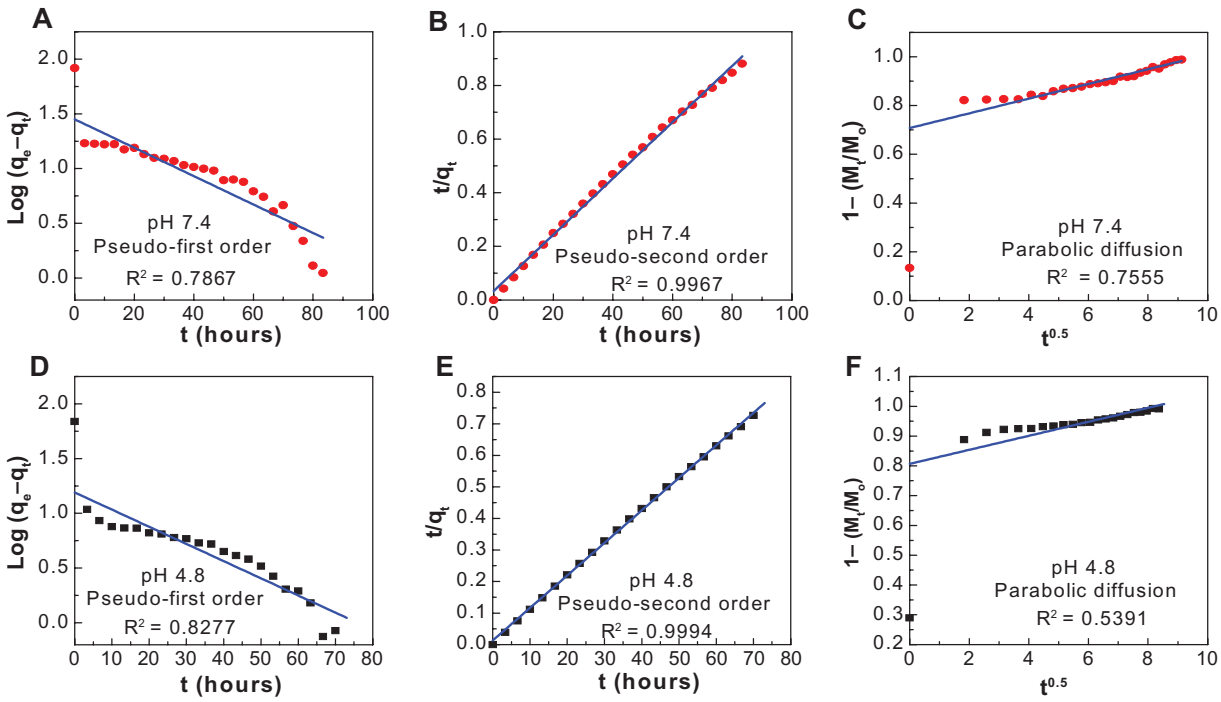

Figure 8 Fitting of the data of cetirizine released from the cetirizine nanocomposite into various solutions to the first-, pseudo-second order kinetics and parabolic diffusion model for pH 7.4 (**A**–**C**) and pH 4.8 (**D**–**F**).

$$\ln (q_e - q_t) = \ln q_e - k_1 t \quad (1)$$

$$t/q_t = 1/k_2 q_e^2 + t/q_e \quad (2)$$

$$(1 - M_t/M_o)/t = k\, t^{-0.5} + b \quad (3)$$

where M_o and M_t are the drug content remaining in the ZLH at release times 0 and t, respectively; q_e and q_t are the equilibrium release amount and the release amount at any time t, respectively; and k is the corresponding release-rate constant.

For the three kinetic models, the results of fitting the experimental data to various kinetic models are given in Figure 8 and Table 3. It was found that the pseudo-second order model gives a better fit for the kinetics of the release of cetirizine from CETN; this result is similar to the kinetic study for the release of camptothecin from another layered double hydroxide.[39] At pH 4.8 (Figure 8E), the correlation coefficient (R^2) and k_2 values are 0.9994 and 0.008 g/mg · h, respectively, compared with 0.9967 and 0.003 g/mg · h, respectively, for pH 7.4 (Figure 8B).

Cytotoxicity of ZLH and CETN nanomaterials

To investigate the cytotoxicity effect of ZLH and CETN nanomaterials toward Chang cells line, we used the Trypan Blue exclusion assay at various nanomaterial concentrations: 7.81, 15.63, 31.25, 62.5, 125, 250, 500, and 1000 µg/mL. The results are shown in Figure 9 and Table 4. In Table 4, it can be seen that the CETNs at concentrations of 500–1000 µg/mL cause some cells death with the IC_{50} 617 µg/mL value, whereas the ZLH shows cytotoxicity with IC_{50} 670 µg/mL.

Effect of cetirizine, CETN, and ZLH on histamine release from RBL-2H3 cells

Increased histamine secretion may be responsible for several clinical symptoms, such as diarrhea, abdominal pain,

Table 3 Correlation coefficient (R^2), rate constant (k), and half time ($t_{1/2}$) obtained by fitting the data of the release of cetirizine from the cetirizine nanocomposite (CETN) into phosphate buffer solution at pH 7.4 and pH 4.8

Aqueous solution	Saturation release (%)	R^2			Pseudo-second order	
		Pseudo-first order	Pseudo-second order	Parabolic diffusion	Rate constant, k (g/mg · h)	$t_{1/2}$ (h)
pH 7.4	96	0.7867	0.9967	0.7555	0.003	3.80
pH 4.8	97	0.8277	0.9994	0.5391	0.008	1.36

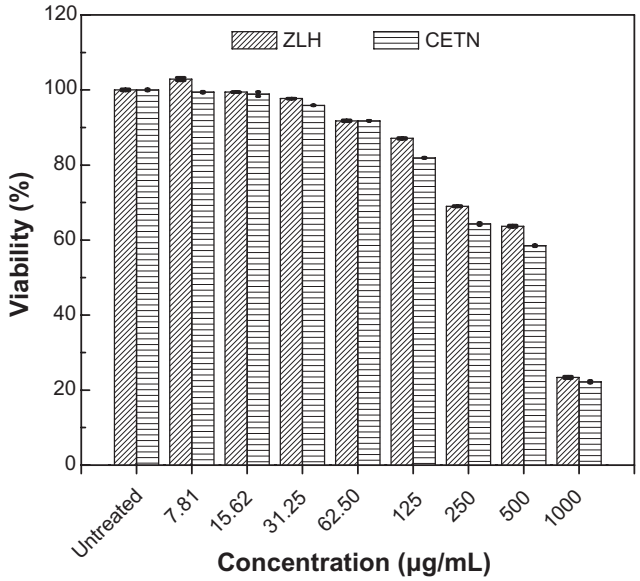

Figure 9 Trypan Blue assays of normal Chang liver cells after 24 hours of treatment with zinc-layered hydroxide (ZLH) and cetirizine nanocomposite (CETN).

and cramping.[42] The antihistamine activities of cetirizine, CETN, and ZLH were evaluated by determining their inhibitory potencies of histamine release in RBL-2H3 cells. Figure 10A–C illustrates the percentage of histamine release in RBL-2H3 cells when treated with cetirizine, CETN, and ZLH. As shown in Figure 10, the effect of the components on histamine release from RBL-2H3 cells was increased as the concentration of the components decreased. However, release of histamine from RBL-2H3 cells was more sensitive to intercalated cetirizine in CETN compared with free cetirizine. It is noteworthy that ZLH has an effect on the histamine release, in that zinc is required to store histamine. A zinc deficiency results in a release of histamines into the surrounding tissue fluids and it is believed that zinc ions prevent most or all of the histamine release by blocking calcium

Table 4 Viability of normal Chang liver cells after 24 hours' treatment with zinc-layered hydroxide (ZLH) and cetirizine nanocomposite (CETN)

Concentrations (µg/mL)	Viability (%)	
	ZLH	CETN
0.00	100.0	100.0
7.81	102.9	99.4
15.62	99.4	98.9
31.25	97.7	95.9
62.5	91.8	91.8
125	87.1	81.9
250	69.0	64.3
500	63.7	58.5
1000	23.4	22.2

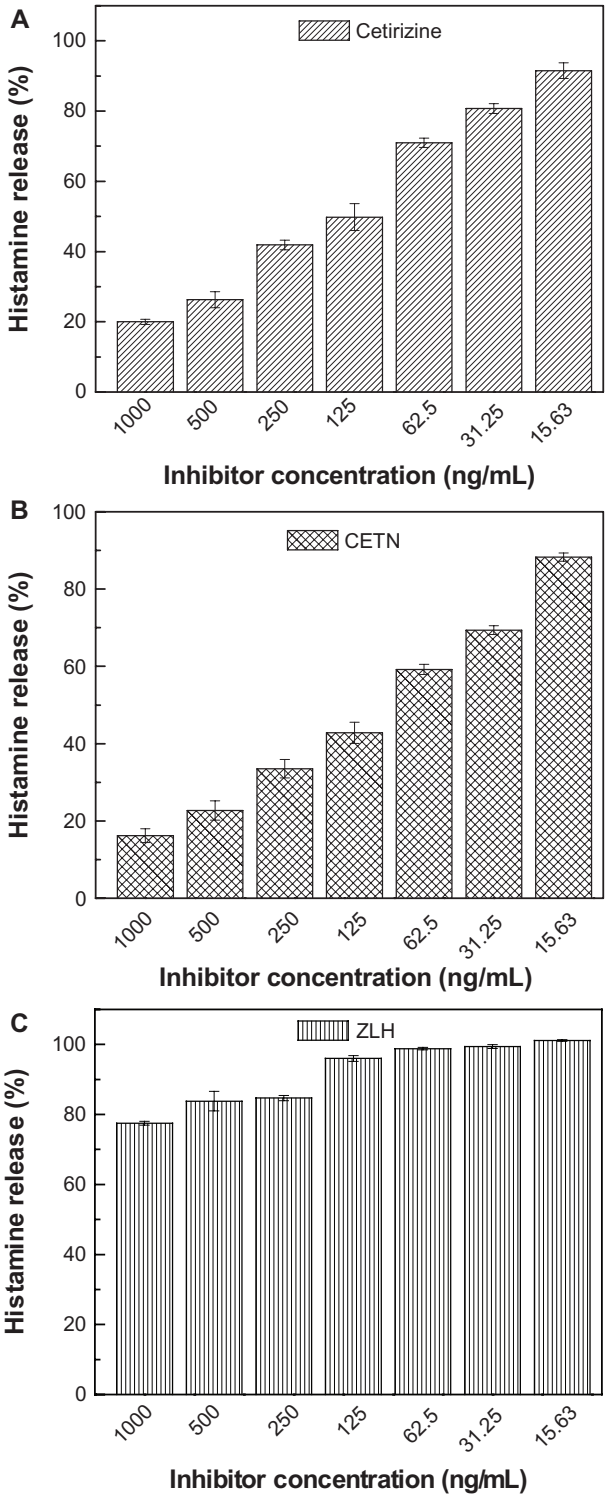

Figure 10A–C Histamine release response of rat basophilic leukemia cells treated at different concentrations of cetirizine, cetirizine nanocomposite, and zinc-layered hydroxide.

uptake induced by anti-IgE activation.[43] The inhibition of histamine release by cetirizine and CETN is shown in Figure 11, with the values of 40.8% and 29.0% for CETN nanocomposite and cetirizine, respectively, at 62.5 ng/mL.

Table 5 Inhibition percentage of histamine release in rat basophilic leukemia cells by free cetirizine, the cetirizine nanocomposite (CETN), zinc-layered hydroxide (ZLH), and cetirizine intercalated into CETN

Concentration (ng/mL)	Inhibition (%)			
	Cetirizine	ZLH	CETN	Cetirizine in CETN*
1000	80.0	22.5	83.8	–
500	73.7	16.2	77.3	67.6
250	58.1	15.3	66.5	62.0
125	50.2	4.0	57.2	62.5
62.5	29.0	1.2	40.8	56.0
31.25	19.3	0.6	30.6	40.2
15.63	8.5	−1.1	11.7	31.7

Note: *Inhibition (%) by intercalated cetirizine into CETN = (inhibition by CETN at 1000 ng/mL – inhibition by ZLH at 500 ng/mL), because the loading of cetirizine into CETN is 49.4%.

The study also shows that after 10 minutes of incubation with CETN, 97.6 ng/mL was enough to reduce the histamine release by up to 50%, compared with 124.4 ng/mL for free cetirizine. However, ZLH at 1000 and 500 ng/mL significantly inhibited histamine release (22.5% and 16.2% inhibition, respectively). Table 5 shows a comparison of the effect of free cetirizine and the intercalated cetirizine toward inhibition of histamine release. The inhibition of histamine release by the intercalated cetirizine at concentrations of 15.63, 31.25, and 62.5 ng/mL was 3.7-, 2.1-, and 1.9-fold higher, respectively, than for free cetirizine. This result demonstrated that intercalated cetirizine has a higher inhibitory effect on histamine release than its counterpart, cetirizine alone. The decrease in histamine content in this work is in good agreement with the results obtained in a previous study,[44] which showed that zinc oxide at relatively low concentrations inhibits in vitro histamine release.

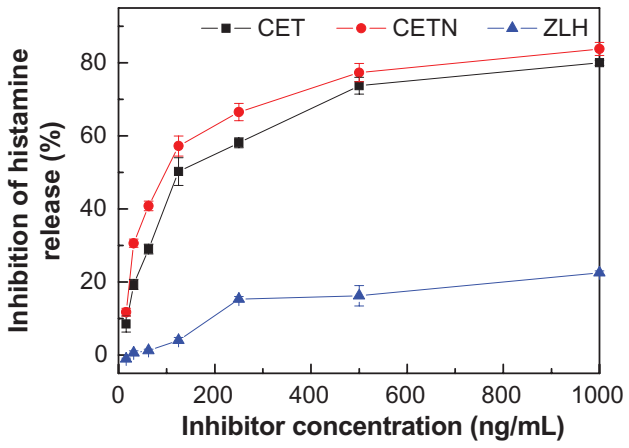

Figure 11 Percentage inhibition of histamine release into rat basophilic leukemia cells at different concentrations of cetirizine (CET), cetirizine nanocomposite (CETN), and zinc-layered hydroxide (ZLH).

Conclusion

In this study, a new, simple, and direct method for the intercalation of anions into ZLH was realized, using zinc oxide as the starting material. The resulting nanocomposite shows long-range, nano-layered structure with high crystallinity. The basal spacing of the nanocomposite was measured as 33.9 Å from the six harmonics observed in the X-ray diffraction patterns with a 49.4% (w/w) loading of the active drug. The orientation of the anion between the interlayers is a horizontal bilayer, with interaction between the negative charge of cetirizine and the positive charge of the inorganic layers. The guest was found to be more thermally stable than its unbound counterpart. The release of cetirizine from CETN occurred in a controlled manner, with 96% released after 83 hours and 97% released after 73 hours at pH 7.4 and 4.8, respectively. The release, in all cases, was governed by pseudo-second order kinetics. The IC_{50} for CETN and ZLH were 617 and 670 µg/mL, respectively. Comparing the antihistamine activity of cetirizine and intercalated cetirizine in CETN in RBL-2H3 cells, the results clearly show that the intercalated cetirizine in the CETN is more potent than cetirizine alone.

Acknowledgment

We thank the Ministry of Higher Education of Malaysia for financial support under grant No FRGS/1/11/5G/UPM/01/2 (Vot 5524165). The author (Samer Hasan) is grateful to Universiti Putra Malaysia for International Graduate Research Fellowship (IGRF).

Disclosure

The authors report no conflicts of interest in this work.

References

1. Mangiacapra P, Raimondo M, Tammaro L, Vittoria V, Malinconico M, Laurienzo P. Nanometric dispersion of a Mg/Al layered double hydroxide into a chemically modified polycaprolactone. *Biomacromolecules*. 2007;8(3):773–779.
2. Louer M, Louer D, Grandjean D. Etude structurale des hydroxynitrates de nickel et de zinc. I. Classification structural [Structural studies of hydroxynitrates nickel and zinc. I. structural classification]. *Acta Cryst B*. 1973;29(8):1696–1703. French.
3. Stahlin W, Oswald HR. The crystal structure of zinc hydroxide nitrate, $Zn_5(OH)_8(NO_3)$ 2.2 H_2O. *Acta Cryst*. 1970;B26(6):860–863.
4. Hussein MZ, Al Ali SH, Zainal Z, Hakim MN. Development of antiproliferative nanohybrid compound with controlled release property using ellagic acid as the active agent. *Int J Nanomedicine*. 2011;6:1373–1383.
5. Kwak SY, Jeong YJ, Park JS, Choy JH. Bio-LDH nanohybrid for gene therapy. *Solid State Ionics*. 2002;151(1–4):229–234.

6. Dan-dan L, Yan L, Xu Y. Detection of biocompatibility between nano-Layered double hydroxides and hela cells. In: *Proceedings of the 3rd International Conference on Bioinformatics and Biomedical Engineering (iCBBE 2009)*, Beijing, People's Republic of China, June 11–16, 2009. Piscataway, NJ: Institute of Electrical and Electronic Engineers, Inc; 2009:1–3.
7. Son SJ, Bai X, Lee SB. Inorganic hollow nanoparticles and nanotubes in nanomedicine: Part 2: Imaging, diagnostic, and therapeutic applications. *Drug Discov Today*. 2007;12(15–16):657–663.
8. Choy JH, Kwak SY, Park JS, Jeong YJ. Cellular uptake behavior of [gamma 32P] labeled ATP-LDH nanohybrids. *J Mater Chem*. 2001;11(6):1671–1674.
9. Soma CE, Dubernet C, Barratt G, et al. Ability of doxorubicin-loaded nanoparticles to overcome multidrug resistance of tumor cells after their capture by macrophages. *Pharmaceut Res*. 1999;16(11): 1710–1716.
10. Hussein MZ, Ghotbi MY, Yahaya AH, Abd Rahman MZ. Synthesis and characterization of (zinc-layered-gallate) nanohybrid using structural memory effect. *Mater Chem Phys*. 2009;113(1):491–496.
11. Al Ali SHH, Al-Qubaisi M, Hussein MZ, Zainal Z, Hakim MN. Preparation of hippurate-zinc layered hydroxide nanohybrid and its synergistic effect with tamoxifen on HepG2 cell lines. *Int J Nanomedicine*. 2011;6:3099–3111.
12. Choy JH, Shin J, Lim SY, Oh JM, Oh MH, Oh S. Characterization and stability analysis of ZnO nanoencapsulated conjugated linoleic acid. *J Food Sci*. 2010;75(6):N63–N68.
13. Cursino AC, Gardolinski J, Wypych F. Intercalation of anionic organic ultraviolet ray absorbers into layered zinc hydroxide nitrate. *J Colloid Interface Sci*. 2010;347(1):49–55.
14. Hwang SH, Han YS, Choy JH. Intercalation of functional organic molecules with pharmaceutical, cosmeceutical and neutraceutical functions into layered double hydroxides and zinc basic salts. *Bull Korean Chem Soc*. 2001;22(9):1019–1022.
15. Rouba S, Rabu P, Drillon M. Synthesis and characterization of new quasi-one-dimensional Mn(II) hydroxynitrates $(Mn_xZn_{1-x})(OH)(NO_3)H_2O$ (x = 0.53, 1.00). *J Solid State Chem*. 1995;118(1):28–32.
16. Newman SP, Jones W. Comparative study of some layered hydroxide salts containing exchangeable interlayer anions. *J Solid State Chem*. 1999;148(1):26–40.
17. Rajamathi Michael, Kamath P. Vishnn. Urea hydrolysis of cobalt (II) nitrate melts: Synthesis of noval hydroxides and hydroxyl nitrate. *Int J Inorg Mater*. 2001;3(7):901–906.
18. Best CH, Dale HH, Dudley HW, Thorpe WV. The nature of the vasodilator constituents of certain tissue extracts. *J Physiol*. 1927;62(4): 397–417.
19. Brown V, Ennis M. Flow-cytometric analysis of basophil activation: inhibition by histamine at conventional and homeopathic concentrations. *Inflamm Res*. 2001;50(2):47–48.
20. Marone G, Columbo M, De Paulis A, Cirillo R, Giugliano R, Condorelli M. Physiological concentrations of zinc inhibit the release of histamine from human basophils and lung mast cells. *Inflamm Res*. 1986;18(1): 103–106.
21. Dobashi K, Iizuka K, Houjou S, et al. Effect of cetirizine on antigen-induced tracheal contraction of passively sensitized guinea pigs. *Ann Allergy Asthma Immunol*. 1996;77(4):310–318.
22. Hussein MZ, Hashim N, Yahaya AH, Zainal Z. Synthesis and characterization of [4-(2, 4-dichlorophenoxybutyrate)-zinc layered hydroxide] nanohybrid. *Solid State Sci*. 2010;12(5):770–775.
23. Xia S-J, Ni Z-M, Xu Q, Hu B-X, Hu J. Layered double hydroxides as supports for intercalation and sustained release of antihypertensive drugs. *J Solid State Chem*. 2008;181(10):2610–2619.
24. Ribeiro C, Arizaga GG, Wypych F, Sierakowski MR. Nanocomposites coated with xyloglucan for drug delivery: In vitro studies. *Int J Pharm*. 2009;367(1–2):204–210.
25. Wang Z, Wang E, Gao L, Xu L. Synthesis and properties of Mg2Al layered double hydroxides containing 5-fluorouracil. *J Solid State Chem*. 2005;178(3):736–741.
26. Stahlin W, Oswald HR. The infrared spectrum and thermal analysis of zinc hydroxide nitrate. *J Solid State Chem*. 1971;3(2):252–255.
27. Xingfu Z, Zhaolin H, Yiqun F, Su C, Weiping D, Nanping X. Microspheric organization of multilayered ZnO nanosheets with hierarchically porous structures. *J Phys Chem C*. 2008;112(31): 11722–11728.
28. Testa B, Pagliara A, Carrupt PA. The molecular behaviour of cetirizine. *Clin Exp Allergy*. 1997;27:13–18.
29. Bora MM. Adsorption of pigment from annatto seed utilizing Fish Scale as biosorbent. *J Chem Pharm Res*. 2010;2(5):75–83.
30. Kenawi IM, Barsoum BN, Youssef MA. Drug-drug interaction between diclofenac, cetirizine and ranitidine. *J Pharm Biomed Anal*. 2005;37(4): 655–661.
31. Yuan Q, Wei M, Evans DG, Duan X. Preparation and investigation of thermolysis of L-aspartic acid-intercalated layered double hydroxide. *J Phys Chem B*. 2004;108(33):12381–12387.
32. Wei M, Guo J, Shi Z, et al. Preparation and characterization of l-cystine and l-cysteine intercalated layered double hydroxides. *J Mater Sci*. 2007;42(8):2684–2689.
33. Miao J, Xue M, Itoh H, Feng Q. Hydrothermal synthesis of layered hydroxide zinc benzoate compounds and their exfoliation reactions. *J Mater Chem*. 2005;16(5):474–480.
34. Arizaga GC, Gardolinski JE, Schreiner WH, Wypych F. Intercalation of an oxalatooxoniobate complex into layered double hydroxide and layered zinc hydroxide nitrate. *J Colloid Interf Sci*. 2009;330(2): 352–358.
35. Huang X, Brazel CS. On the importance and mechanisms of burst release in matrix-controlled drug delivery systems. *J Control Release*. 2001;73(2–3):121–136.
36. Tyner KM, Schiffman SR, Giannelis EP. Nanobiohybrids as delivery vehicles for camptothecin. *J Control Release*. 2004;95(3):501–514.
37. Hou WG, Jin ZL. Synthesis and characterization of Naproxen intercalated Zn-Al layered double hydroxides. *Colloid Polym Sci*. 2007;285(13):1449–1454.
38. Wei M, Pu M, Guo J, et al. Intercalation of l-Dopa into Layered Double Hydroxides: Enhancement of Both Chemical and Stereochemical Stabilities of a Drug through Host-Guest Interactions. *Chem Mater*. 2008;20(16):5169–5180.
39. Liu C, Hou W, Li L, Li Y, Liu S. Synthesis and characterization of 5-fluorocytosine intercalated Zn-Al layered double hydroxide. *J Solid State Chem*. 2008;181(8):1792–1797.
40. Dong L, Yan L, Hou WG, Liu SJ. Synthesis and release behavior of composites of camptothecin and layered double hydroxide. *J Solid State Chem*. 2010;183(8):1811–1816.
41. Ho YS, Ofomaja AE. Pseudo-second-order model for lead ion sorption from aqueous solutions onto palm kernel fiber. *J Hazard Mater*. 2006;129(1–3):137–142.
42. Kong X, Shi S, Han J, Zhu F, Wei M, Duan X. Preparation of glycy-l-tyrosine intercalated layered double hydroxide film and its in vitro release behavior. *Chem Eng J*. 2010;157(2–3):598–604.
43. Wood JD. Enteric neuroimmuno physiology and pathophysiology. *Gastroenterology*. 2004;127:635–657.
44. Marone G, Findlay SR, Lichtenstein LM. Modulation of histamine release from human basophils in vitro by physiological concentrations of zinc. *J Pharmacol Exp Ther*. 1981;217(2):292–298.
45. Ou D, Li D, Cao Y, et al. Dietary supplementation with zinc oxide decreases expression of the stem cell factor in the small intestine of weanling pigs. *J Nutr Biochem*. 2007;18(12):820–826.

International Journal of Nanomedicine

Dovepress

Publish your work in this journal

The International Journal of Nanomedicine is an international, peer-reviewed journal focusing on the application of nanotechnology in diagnostics, therapeutics, and drug delivery systems throughout the biomedical field. This journal is indexed on PubMed Central, MedLine, CAS, SciSearch®, Current Contents®/Clinical Medicine, Journal Citation Reports/Science Edition, EMBase, Scopus and the Elsevier Bibliographic databases. The manuscript management system is completely online and includes a very quick and fair peer-review system, which is all easy to use. Visit http://www.dovepress.com/testimonials.php to read real quotes from published authors.

Submit your manuscript here: http://www.dovepress.com/international-journal-of-nanomedicine-journal